ESMO GOOD SCIENCE BETTER MEDICINE BEST PRACTICE

IOTECH IMMUNO-ONCOLOGY AND TECHNOLOGY

ORIGINAL ARTICLE

Rational engineering of an improved adenosine deaminase 2 enzyme for weaponizing T-cell therapies

J. R. Cox, M. Jennings, C. Lenahan, M. Manion, S. Courville & J. Blazeck*

School of Chemical and Biomolecular Engineering, Georgia Institute of Technology, Atlanta, USA

Available online 28 June 2023

Adenosine is a potent immunosuppressive metabolite that accumulates in the extracellular space within solid tumors and inhibits the antitumor function of native immune cell responses as well as chimeric antigen receptor (CAR) T-cell therapies. Here, we show that engineered human cells can degrade extracellular adenosine through secretion of adenosine deaminase (ADA) enzymes—a possible therapeutic enhancement for CAR T cells. We first determine that the high-activity ADA1 isoform is naturally intracellularly restricted and show that the addition of canonical or computationally predicted secretory peptides did not allow for improved secretion. We did, however, determine that the lower-activity ADA2 isoform is naturally secreted. Thus, we utilized phylogenetic-based structural comparisons to guide a mutational survey of ADA2 active site residues, which when coupled with a high-throughput screen for enhanced ADA2-mediated extracellular adenosine rate allowed isolation of the most catalytically efficient ADA2 variant reported to date. When expressed by human cells, this variant exhibits 30× higher extracellular adenosine degradation activity than the wild-type enzyme. Finally, we demonstrate that Jurkat and CAR T cells engineered to express this secreted, high-activity ADA2 variant can degrade significant amounts of extracellular adenosine *in vitro*.

Key words: T-cell therapy, immunotherapy, checkpoint inhibition, protein engineering

INTRODUCTION

Chimeric antigen receptor (CAR) T-cell therapies have demonstrated groundbreaking success in the treatment of blood-based cancers. Unfortunately, CAR T efficacy against solid tumor indications has been limited, in part due to the immunosuppressive tumor microenvironment (TME).[1] Recently, engineering T-cell therapies to be 'armored' against the immunosuppressive TME has been shown to increase their antitumor function.[2] To date, most T-cell 'armor' has been designed to enable their resistance to receptor-mediated or cytokine-mediated immune (i.e. protein-mediated) checkpoints [e.g. secrete α-programmed cell death protein 1 (PD-1) single-chain variable fragments (scFvs) or interleukin (IL)-12].[3-7] While such approaches are promising, T cells face additional immunosuppressive barriers in the TME, such as the accumulation of inhibitory small-molecule metabolites like adenosine.[8]

Adenosine is a ribonucleoside that inhibits the function of immune cells, including T cells.[8] Adenosine has been shown to potently inhibit T-cell function by signaling through the adenosine receptors $A_{2A}R$ and $A_{2B}R$ to promote the intracellular accumulation of cyclic adenosine monophosphate and activate protein kinase A (cAMP/PKA) pathway (also known as the adenosinergic pathway).[8] Foundational studies demonstrated that $A_{2A}R$ agonism accumulates suppressive cAMP within immune cells as a critical negative feedback mechanism for attenuating systemic or tissue-specific immune response *in vivo*.[9] Seminal studies in murine tumor models demonstrated that this pathway is co-opted by tumor tissue, helping give rise to the paradoxical coexistence of tumoral and antitumor T cells.[10] Importantly, it was further shown that antagonism of $A_{2A}R$ with ZM241385 could slow tumor growth in mice, pinpointing $A_{2A}R$ specifically, and potentially the entirety of the adenosinergic pathway more broadly, as key clinical targets for immune-oncology.[10] Furthermore, a state-of-the-art $A_{2A}R$ antagonist ciforadenant has demonstrated efficacy in refractory renal cell cancer patients, particularly patients with an adenosine-regulated pre-treatment gene signature.[11]

Extracellular adenosine is generated from ATP by ecto-enzymes (CD39, CD73, TRACP, TNAP, PLAP, etc.) to reach concentrations of 100 μM in tumors compared to

*Correspondence to: Prof. John Blazeck, School of Chemical and Biomolecular Engineering, Georgia Institute of Technology, 311 Ferst St. NW, Atlanta, GA 30332, USA. Tel: +404-894-2000

E-mail: john.blazeck@chbe.gatech.edu (J. Blazeck).

physiological nanomolar ranges.[12] Following important studies implicating the role of adenosine synthesis enzymes CD39 and CD73 in immune suppression and overall tumor progression, monoclonal antibody therapeutics and inhibitors were designed to target these enzymes.[13] Blockade therapy targeting CD73 has been very promising, and it synergizes well with other immunotherapeutic antagonists [e.g. cytotoxic T-lymphocyte-associated protein-4 (CTLA-4)].[14-16] Overall though, blockade therapies exhibit varying degrees of efficacy, due to the redundancies in adenosine generation/signaling and the unpredictable tumor presence of antitumor T cells, making adoptive cell therapy and tumoral adenosine depletion a logical extension to augment therapies targeting the adenosinergic pathway.[12,17] To this end, the CRISPR-Cas9-mediated knockout of the $A_{2A}R$ was recently shown to partially rescue CAR T-cell function in solid tumor preclinical models.[18] Thus, we sought to develop a method to engineer T cells to overcome adenosine-mediated immune suppression via enzymatic adenosine depletion. In this manner, T cells might overcome the immunosuppressive adenosinergic axis, despite adenosine synthesis redundancies.

Adenosine deaminase (ADA) therapy, traditionally used in ADA deficiency, was hypothesized to be a therapeutic solution to overcoming adenosine-mediated immune suppression early on by Sitkovsky and colleagues.[8] ADA enzymes can irreversibly deaminate adenosine into inosine, a metabolite that binds $A_{2A}R$ with $\sim$1000$\times$ weaker affinity.[19] Inosine has been implicated as an immunosuppressant in certain contexts, though these *in vitro* studies may have been carried out at supraphysiological levels.[20-22] More recently, inosine has been also shown to have a role in pro-inflammatory T-cell effector functions by supporting T_{H1} cell differentiation during activation.[23] In addition, inosine (but not adenosine) can serve as an alternative carbon source for glucose-restricted T cells in tumors.[24]

Humans have two ADA isoforms: a primarily intracellular variant, ADA1, that is ubiquitously expressed and a secreted variant, ADA2, that is found in serum and expressed by myeloid cells.[25,26] ADA1 is considerably more active than ADA2 as it has a higher k_{cat} ($\sim$190 s^{-1} compared to 45 s^{-1}) and nearly 100-fold lower K_M (26 μM compared to 2 mM).[25,26] Other than its role in purine salvage, ADA1 moonlights as a positive regulator of lymphocyte activation, adhesion, and differentiation via interaction with surface protein CD26.[27-29] ADA2 may have a role in clearing elevated extracellular adenosine concentrations, but has other roles in monocyte−macrophage differentiation and CD4+ T-cell proliferation, both of which are largely independent of its ADA activity.[30,31] Adenosine depletion with ADA has had recent success in practice, in which ADA1 or an engineered ADA2 was shown to promote T-cell antitumor function in solid tumors.[8,32-34] An ADA2 enzyme could reduce adenosine levels below the affinity threshold of $A_{2A}R$ for adenosine (between 25 and 250 nM) for up to 24 h, despite having a much higher K_M of 1 mM.[33,35]

In this work, we developed a way to engineer human cells, including CAR T cells, to allow them to remodel the tumoral extracellular metabolic environment and eliminate the immunosuppressive adenosine metabolite. Firstly, we showed that despite being largely intracellular restricted, constitutive ADA1 expression in HEK293 cells results in superior extracellular adenosine deamination activity than the naturally secreted ADA2 enzyme, due to ADA1's higher activity. Surprisingly, we were unable to improve ADA1 secretion, despite the introduction of an either canonical or computationally predicted N-terminal signal peptides or Fc-fusions. Therefore, to improve the ability of an engineered cell to degrade extracellular adenosine, we engineered human ADA2 variants with more favorable kinetic properties. By generating a library of ADA2 variants based on a phylogenetic analysis of eukaryotic homologs, and developing a complementary reverse transfection-based high-throughput screen for extracellular ADA activity, we were able to isolate an improved ADA2 variant with an approximate sevenfold reduction in K_M ($\sim$2 mM-$\sim$0.3 mM) that is more active at tumoral adenosine concentrations. Finally, we demonstrated that both Jurkat and CAR T cells can secrete the enzyme. These results suggest that engineering T cells with ADA2 (or a variant thereof) could be a strategy to directly deplete adenosine in solid tumors to improve T-cell and bystander immune cell function. In future work, ADA2-engineered T cells will be tested in a suitable preclinical tumor model to determine whether they rescue adenosine-mediated T-cell dysfunction *in vivo*.

MATERIALS AND METHODS

Cell lines and cultivation

HEK293T cells were maintained in GlutaMAX and 10% fetal bovine serum (FBS) from Gibco™ (Grand Island, NY). Jurkat cells were cultured in RPMI-1640 (Gibco™) supplemented with 10% FBS. All cell lines used in this study were tested for mycoplasma and verified negative.

Plasmid and ADA2 library construction

ADA1 and ADA2 human code determining sequences were ordered as double-stranded gene fragments (with 6xHis tags to ease detection) from Twist Bioscience (San Francisco, CA). All ADA2 and ADA1 T2A-GLuc constructs were amplified via PCR and inserted into a pcDNA3 backbone via Gibson assembly. ADA2wt and ADA2v20 expression constructs for protein purification were PCR'd and assembled into a pcDNA3.1 backbone without a T2A-GLuc sequence via Gibson assembly. All lentiviral constructs were constructed via Gibson assembly and inserted into a pLeGO-C backbone (Addgene #27348; Watertown, MA) digested with XbaI and EcoRI (New England Biolabs®; Ipswich, MA).

For the ADA2 variant library construction, a base construct containing Esp3I sites upstream of the T2A-GLuc sequence was first constructed from a pcDNA3 backbone via Gibson assembly. ADA2 mutations were introduced by using degenerate primers that, following PCR, resulted in eight

ADA2 fragments that harbored the desired mutations. Next, the fragments were added to the same PCR reaction at equimolar concentrations (normalized by mutations per fragment) and amplified without primers via overlap extension PCR. A final amplification of the re-assembled ADA2 variant library amplicon followed that also added Esp3I overhangs for ligation into the final backbone construct. A full primer table can be found in Supplementary Table S1, available at https://doi.org/10.1016/j.iotech.2023.100394.

Using standard electroporation protocols, lentiviral and retroviral plasmids were transformed into NEB® Stable *Escherichia coli*, while all plasmids with pcDNA backbones were transformed into *E. coli* strain NEB® 10β.[36] All plasmids were sequence confirmed via Sanger sequencing before use, and plasmids used for transfection were maxiprepped with PureLink™ HiPure Plasmid Maxiprep Kit (Invitrogen™ K210007; Waltham, MA).

Adenosine kinetic assays in supernatant and cell lysates

For adenosine kinetic assay experiments from cell supernatants, HEK293T cells were transiently transfected in 12-well plates with 1 μg of plasmid DNA with TransIT-LT1 transfection reagent (MirusBio, MIR 2305; Madison, WI) according to the manufacturer's instructions. Twenty-four hours post-transfection, the media were changed to serum-free media. Another 24 h later, the cultured media were taken and spun at 1000 × *g* for 5 min to pellet detached cells and 1 ml of supernatant harvested. Adhered cells were washed once with phosphate-buffered saline (PBS)−/− pH = 7.4 and lysed with 300 μL of M-PER™ protein extraction reagent (Thermo Scientific™ #78501; Waltham, MA) supplemented with Halt™ protease inhibitor cocktail (Thermo Scientific™ #78442) for 5 min with gentle agitation. Lysed cells were centrifuged at 14 000 × *g* for 5 min and the soluble proteins harvested. Forty microliters of supernatant or lysate sample was pipetted into UV-Star® 96-well plates (VWR; Radnor, PA). One hundred and sixty microliters of PBS solution with indicated adenosine concentrations was added to each well and an absorbance of 260 nm was tracked with a SynergyHTX microplate reader for 30 min. Adenosine degradation rates were obtained by analyzing the initial linear region of the resulting slope and adjusting for in-plate dilutions. Lysate degradation rates were divided by 10/3 to account for volume equivalences with supernatant for comparison. Standard curves were generated with serum-free cell culture media.

For Jurkat cell experiments, 10^6 cells/ml were seeded in 12-well plates (1 ml culture volume). Forty-eight hours post-seeding, cells were spun at 500 × *g* for 5 min and supernatant harvested. In-plate kinetic analysis for Jurkat cells was the same as described for HEK293T cells above, but with the proper cell culture media (RPMI-1640 and 10% FBS) for standard curves. For primary T-cell experiments, 10^6 cells/ml were seeded in 96-well plates and processed the same way as previously described.

Sodium dodecyl sulfate–polyacrylamide gel electrophoresis (SDS-PAGE) and western blot

For western blot experiments, HEK293T cells were transfected with the indicated DNA construct in 12-well plates as previously described. Twenty-four hours post-transfection, media were changed to serum-free media. After another 24 h, supernatant was sampled and supplemented with Halt™ protease inhibitors. Cells were washed once with PBS−/− and lysed with M-PER™ protein extraction reagent (supplemented with Halt™ protease inhibitor cocktail) for 5 min with gentle agitation. Lysed cells were centrifuged at 14 000 *g* for 5 min and the soluble proteins harvested and stored at −80°C until blotting. Protein concentrations of supernatants were assessed by Bradford assay (Bio-Rad; Hercules, CA). For lysates, 3 μg of protein and for supernatants 1 μg of protein were denatured with Bond-Breaker™ TECP (Thermo Scientific™, #77720) and 2x Laemmli sample buffer (Bio-Rad, #1610737) according to the manufacturer's instruction loaded into each well of a NuPAGE™ 4%-12% Bis-Tris gel (Invitrogen™, #NP0322BOX). The SDS-PAGE gel was run on an Invitrogen™ Mini Gel Tank at 200 V for 20 min in 1x MES buffer (Invitrogen™, NP0002). Polyvinylidene difluoride (PVDF) membranes (Thermo Scientific™, #88520) were activated with methanol (Sigma-Aldrich; St. Louis, MO) for 5 min, and then proteins transferred to the membrane in Bolt™ Transfer Buffer (Invitrogen™, #BT00061) supplemented with 10% methanol and 1 : 1000 NuPAGE™ antioxidants (NP0005) at 30 V for 90 min. The membrane was then washed with PBS−/− with 0.1% Tween 20 (Sigma-Aldrich, #P9416-100ML) 3× for 5 min, and then blocked for an hour at room temperature with Odyssey blocking buffer (LI-COR, #927-70001; Lincoln, NE). After blocking, the membrane was washed 3× for 5 min with PBS and Tween again, and then stained with 1 : 250 diluted primary antibodies (R&D Systems, mouse α-His: MAB050-SP, rabbit α-GAPDH: 2275-PC-020; Minneapolis, MN) in blocking buffer with 0.02% Tween 20 overnight at 4°C. The following morning, the membranes were washed 3× for 5 min with PBS and 0.1% Tween, and then secondary antibodies [LI-COR, goat α-mouse immunoglobulin G (IgG): #926-32210, goat α-rabbit: #926-68071] were added at 1 : 10 000 dilutions in blocking buffer with 0.02% Tween. After another 3× wash step, the membrane was imaged on an Odyssey® DLx imager.

ADA2 library screening

For library screening, ADA2 constructs were tested through HEK293T reverse transfection. In brief, DNA colony picks were miniprepped (Qiagen) and normalized to a concentration of 100 ng/μL. Four hundred nanograms of each DNA construct was pipetted into a flat bottom tissue culture (TC)-treated 96-well plate. Then, prediluted TransIT-LT1 and Opti-MEM solution was added to each well according to the supplier's reverse transfection protocol. Finally, 5 × 10^4 HEK293T cells were pipetted into each well and incubated. Forty-eight hours post-transfection, 40 μL of supernatant

was transferred to UV-Star® 96-well plates (VWR) for adenosine kinetic assays. Twenty microliters of supernatant was reserved for Gaussia luciferase (GLuc) assays with the Pierce™ Gaussia Luciferase Assay (Thermo Scientific™ #16161) in white 96-well plates (VWR), according to the manufacturer's instructions.

ADA2 protein expression and purification

A total of 4×10^6 HEK293T cells were seeded into a 10-cm dish. The next day, 10 μg of pcDNA3.1 vectors coding for ADA2wt or ADA2v20 was transfected with TransIT-LT1 according to the manufacturer's instruction. Twenty-four hours post-transfection, the media were vacuumed off and replaced with serum-free GlutaMAX. Twenty-four hours after the media change, the supernatant was spun at $1000 \times g$ for 5 min, then filtered through a polyethersulfone (PES) 0.2-μm filter (VWR), and supplemented with Halt™ protease inhibitor cocktail. Next, the supernatant was diluted 1 : 2 with PBS−/− pH = 7.4 and transferred to a superloop. An AKTA Pure 25 fixated with a HisTrap Excel Ni-Sepharose (GE, GE17-3712-06; Boston, MA) 1 ml column encased in a 4°C refrigerator was equilibrated with 5 column volumes (CVs) of equilibration buffer (20 mM sodium phosphate, pH = 7.4, 300 mM NaCl). Next, the superloop was loaded (1 ml/min), and washed with 5 CVs of wash buffer (20 mM sodium phosphate, pH = 7.4, 300 mM NaCl, 5 mM imidazole). Bound proteins were eluted (elution buffer, 20 mM sodium phosphate pH = 7.4, 300 mM NaCl, 500 mM imidazole) with a linear gradient (0%-100% wash buffer → elution buffer) up to 5 CVs. One-milliliter fractions containing elution peaks were pooled and desalted with 5 CVs of UPW (Milli-Q), 5 CVs of PBS−/− pH = 7.4, and then the samples were applied and collected after another 2 ml PBS−/− pH = 7.4 wash. Finally, the cleaned and diluted samples were transferred to an Amicon® 30K centrifugal filter (VWR) and centrifuged at 4°C and $4000 \times g$ to concentrate.

Adenosine kinetic assays of purified variants

For kinetic parameter assessment of purified ADA2wt and ADA2v20, a similar protocol was followed from Ma et al.[25] In brief, enzymes were diluted in PBS−/−, pH = 7.4. Forty microliters of diluted enzyme was pipetted into 96-well plates and then 160 μL of titrated adenosine-PBS solutions was added to analyze A_{260} decrease over 5 min. The initial linear region was taken and adjusted for the in-plate dilution. Standard curves were generated by diluting adenosine solutions in PBS. Michaelis−Menten curve fits and resulting k_{cat}/K_M parameters were determined with OriginPro 2021 using the equation given below. Curve fits and R^2 values can be found in Supplementary Figure S1, available at https://doi.org/10.1016/j.iotech.2023.100394.

$$v = \frac{V_{max}[S]}{K_M + [S]}$$

Viral preparation and transduction

For lentiviral preparation, 4×10^6 HEK293T cells were seeded in a 10-cm TC-treated dish. The next day, the HEK293T cells were transfected with 5 μg of transfer vector, 1 μg of pMD2.G (Addgene #12259), and 4 μg of psPAX2 (Addgene #12260) with TransIT-LT1 according to the manufacturer's instructions (pMD2.G and psPAX2 were a gift from Dr. Gabe Kwong). After 48 h, supernatants were spun at $1000 \times g$ for 5 min to pellet detached cells. Supernatant was then filtered through 0.45-μm PES filters and then precipitated with PEG-*it*™ viral precipitation solution (SBI, LV825A-1; Palo Alto, CA) according to the manufacturer's instructions. Precipitated virus was resuspended in ice-cold PBS−/− (Gibco™) and stored at −80°C until use. For transduction, 1×10^6 Jurkat cells/ml were spinoculated ($2000 \times g$, brakes off) for 90 min in media containing virus with 8 μg/ml polybrene (Sigma-Aldrich, #TR-1003). Twenty-four hours after spinoculation, transduced cells were resuspended in fresh media. For retroviral production, 5×10^6 HEK293T cells were seeded in a 10-cm dish. The next day, 3.3 μg of pCL-Eco and 6.7 μg of retroviral transfer vector (pMKO and pCL-Eco were both a gift from Dr Gabe Kwong) were transfected using TransIT-LT1 according to the manufacturer's instructions. After 48 h, supernatants were spun at $1000 \times g$ for 5 min to pellet detached cells, and then filtered through 0.45-μm PES filters to be precipitated using Retro-Concentin viral precipitation solution (SBI, RV100A-1). Media were added back to the transfected HEK293T cells for a second harvest. Precipitated virus was resuspended in primary mouse T-cell media [RPMI-1640, 3% ATOS, 100 IU/ml IL-2 (Roche; Basel, Switzerland), 100 IU Pen-Strep] and used immediately. The second harvest was carried out 24 h later.

Primary mouse CAR T-cell generation

Spleens from BALB/cJ mice were dissociated with the back end of a syringe into 5 ml of primary mouse T-cell media (RPMI-1640 + 10% FBS, 3% ATOS, 100 IU/ml Pen-Strep, 100 IU/ml rhIL-2 from Roche) and strained through a 45-μm cell strainer (VWR). Red blood cells were lysed using RBC Lysis Buffer (BioLegend, #420302; San Diego, CA) according to the manufacturer's instructions). After isolation, splenocytes were activated using 4 μg/ml of concanavalin A overnight. The next day, 1×10^6 activated T cells were resuspended in 125 μl of retrovirus and 8 μg/ml of polybrene-containing media within 96-well round bottom plates (VWR) and spinoculated at $2000 \times g$ for 90 min. After spinoculation, the T cells were washed and plated in complete media overnight. The next day, T cells were spinoculated a second time using the second harvest of the retroviral supernatant. Transduced CAR T cells were then used 2 days later for downstream experiments. BALB/cJ mice from Jackson Laboratories (Bar Harbor, ME) were maintained at Georgia Tech in pathogen-free, ventilated cages with irradiated food and autoclaved water. Institutional Animal Care and Use Committees at Georgia Tech

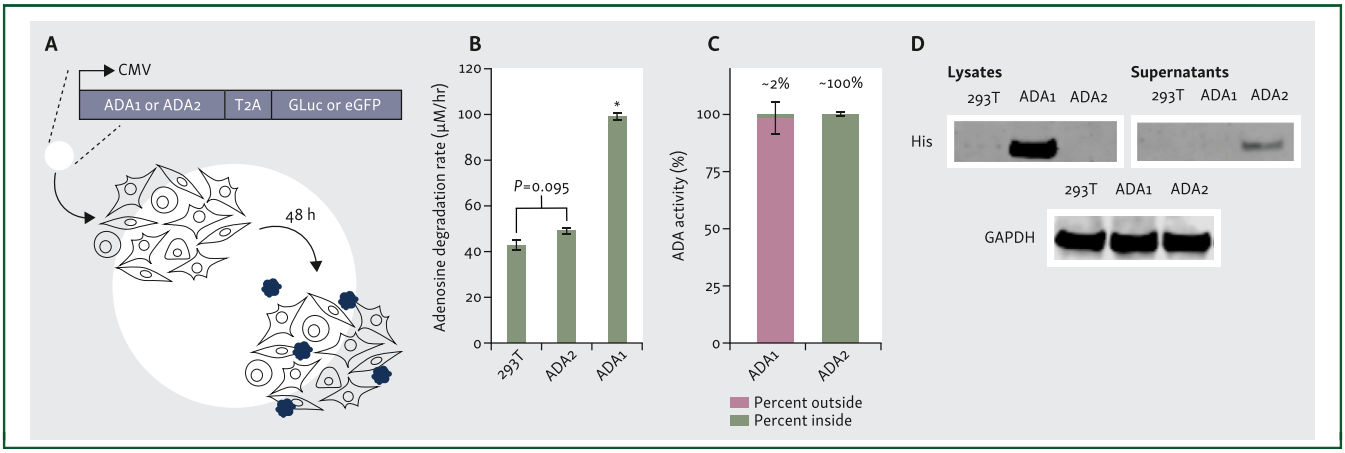

Figure 1. Comparison of extracellular adenosine degradation by adenosine deaminase 1 (ADA1) or ADA2. (A) Experimental schematic showing how extracellular adenosine degradation rate mediated by ADA1 or ADA2 expression was determined after their transfection into HEK293T cells. (B) After 2 days, ADA1 supernatant adenosine degradation is higher than ADA2. Bars represent mean of $n = 3$ independent tests and error bars denote standard error of the mean (SEM). (C) Percent representation of ADA activity within each transfected sample. Green represents the portion of adenosine deaminase activity measured in supernatant (outside of the cells), while red represents the percent activity in cell lysates (inside the cell). Bars are the mean of $n = 3$ independent tests and error bars represent SEM. (D) Western blots of cell lysate and supernatant for untransfected 293T cells and ADA1/ADA2-transfected cells. GAPDH was used as a housekeeping gene. *$P < 0.01$ by Tukey's honestly significant difference (HSD) test.

approved experimental procedures, and housing conditions for mice were as follows: 12 light/12 dark cycle, 65-75°F temperature, and 40%-60% relative humidity. Mice were monitored daily. Mice were euthanized by CO_2 asphyxiation and cervical dislocation before spleen harvest or after showing signs of distress.

RESULTS

Engineering human cells for extracellular adenosine degradation

To establish whether ADA1 and ADA2 would be superior to degrade extracellular adenosine, we transfected HEK293T cells with pcDNA3 vectors encoding either ADA1 or ADA2 under the control of the cytomegalovirus (CMV) promoter. The ADA1/2 coding sequences were followed by a T2A peptide and a GLuc or enhanced green fluorescent protein (eGFP) to allow for normalization based on transfection efficiency (Figure 1A). Two days after transfection, we added adenosine at a final concentration of 250 μM to cell culture supernatant to assay for extracellular ADA activity. Similarly, we tested cell lysate for ADA activity to ascertain intracellular ADA activity. While ADA1-mediated extracellular adenosine degradation surpassed that of wild-type ADA2 (~60 μM/h versus ~7 μM/h in the supernatant), only ~2% of ADA1 was secreted outside of the cells, compared to ~100% of ADA2 (Figure 1B and C). We confirmed these enzymes' tendency toward extracellular secretion or intracellular retention by western blotting of ADA1 and ADA2 expressing HEK293T lysate and supernatant (Figure 1D, Supplementary Figure S2, available at https://doi.org/10.1016/j.iotech.2023.100394). ADA1 was detectable in cell lysate but not in supernatant, while ADA2 was detectable only in supernatant. We concluded that the higher ADA1 extracellular ADA activity compared to ADA2 occurs because ADA1 has a >100× catalytic efficiency (k_{cat}/K_M) than ADA2.[25,26] Thus, even a small percentage (2%) of ADA1 escaping cells are more effective than ADA2 at degrading extracellular adenosine. Experiments were initiated with >95% viability cell cultures to minimize the likelihood of ADA being released from dying cells.

Signal peptides and fusion partners do not improve secretion of the higher-activity ADA1 enzyme

As the ADA1 enzyme showed superior extracellular adenosine degradation activity despite being largely intracellularly restricted, we sought to improve its secretion via protein engineering. Firstly, we sought to augment ADA1 secretion by fusing it to secretory signal peptides (SSPs) (Figure 2A). SSPs are short, ~15-35 amino acid sequences found in the N-terminus of secreted proteins that are cleaved post-translationally or co-translationally during insertion of the nascent polypeptide into the endoplasmic reticulum, allowing proteins to enter the canonical secretion pathway.[37] It has been shown that intracellular proteins can be engineered to be secreted by fusing them with an efficiently cleaved SSP and the efficacy of protein secretion can be improved by using better signal peptides.[37,38]

To select SSPs that would enhance ADA1 secretion, we first carried out an *in silico*, genome-wide scan for optimal SSP—ADA1 fusions. More specifically, we fused every human SSP taken from a signal peptide database (http://www.signalpeptide.de/) to ADA1 protein sequence (without the initiating methionine) *in silico*, and then predicted the cleavage efficiency and localization profile of each SSP—ADA1 sequence using SignalP 5.0 and DeepLoc (Figure 2B).[39,40] SignalP 5.0 predicts signal peptide cleavage using conditional random field classification and transfer learning, while DeepLoc estimates subcellular localization using recurrent neural networks.[39,40] We then selected and constructed several SSP—ADA1 fusion proteins with the highest predicted likelihood for extracellular secretion, as

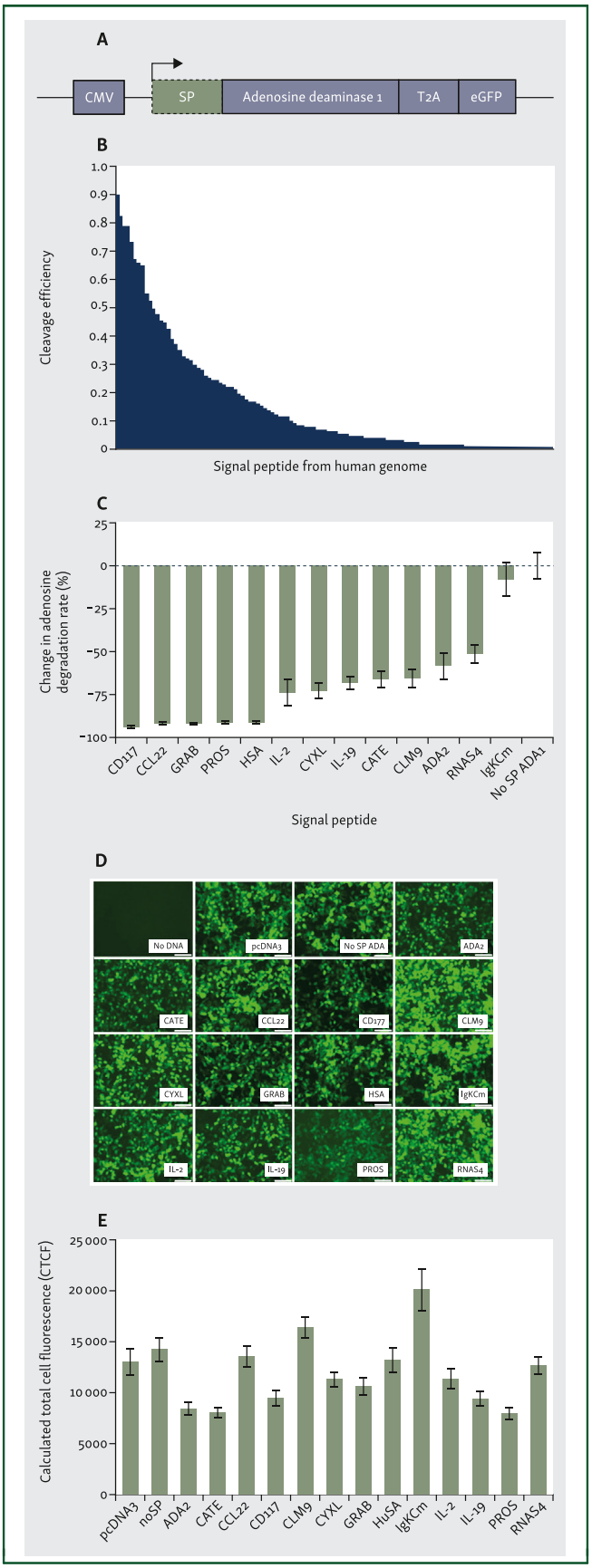

Figure 2. Secretory peptides fail to export adenosine deaminase 1 (ADA1). (A) Construct depiction showing how ADA1 and ADA2 expression was driven by a cytomegalovirus (CMV) promoter and preceded by the indicated signal peptide (SP) sequence. (B) Plot of SP cleavage efficiencies of *in silico* screened SPs (n = 956 SPs) using SignalP. Black bars represent the cleavage efficiency. (C) *In vitro* extracellular adenosine degradation rate of N-terminal fused SP—ADA1 constructs. SP performance with ADA1. Bars represent mean of n = 3 independent tests of the percent change in adenosine degradation rate compared to ADA1 without an SP, and error bars denote standard error of the mean (SEM). (D) Representative images of eGFP after SP—ADA1 constructs show high and uniform transfection efficiency (80%- ~ 100%). White scale bars on the lower right of each panel show 100 μm. (E) ImageJ calculated total cell fluorescence (CTCF), depicting levels of eGFP expression. Bars represent the mean of each cell and errors bars represent SEM.

well as sequences with varying degrees of predicted cleavage efficiency and extracellular localization (Table 1). We further constructed an experimentally verified modified immunoglobulin kappa (mIgκ) signal peptide—ADA1 fusion protein, as the Igκ SSP is routinely used to enhance protein secretion and this modified variant has been shown to allow greater cleavage efficiencies compared to the wild-type sequence.[38]

Surprisingly, all SSP—ADA1 combinations reduced the ADA activity detected in HEK293T-transfected culture supernatant, compared to the unmodified ADA1 (Figure 2C), despite exhibiting similar transfection efficiencies by eGFP expression (Figure 2D). Degradation of adenosine in cell lysate correlated with supernatant degradation rates, suggesting that if the SSP—ADA1 transcripts were translated, they were much more likely to remain intracellular than be secreted (Supplementary Figure S3, available at https://doi.org/10.1016/j.iotech.2023.100394).

We hypothesized that signal peptide cleavage could be failing if ADA1's innate protein structure was preventing access to the cleavage site. Therefore, we added extra amino acid residues in the form of glycine serine linkers (GS), 3x Flags (F), and Tev protease sites (T) between an IgG signal peptide and ADA1, all of which were unsuccessful in augmenting ADA1 secretion (Supplementary Figure S4A, available at https://doi.org/10.1016/j.iotech.2023.100394). We also designed constructs with IgG—Fc fusion partners (for stability) or other small protein fusion partners (to capitalize on their known ability to access alternative signal peptide cleavage pathways), but these were also unsuccessful toward improving ADA1 secretion (Supplementary Figure S4B, available at https://doi.org/10.1016/j.iotech.2023.100394).[41]

Engineering ADA2 to enhance its catalytic activity

Because ADA1 secretion could not be improved, we sought to engineer the lower-activity ADA2 isoform to have improved kinetic parameters as it is natively secreted into the cell culture supernatant (Figure 1). At the entry gate of the active site, ADA2 has many hydrophilic amino acid residues compared to other phylogenetic homologs, which have more hydrophobic gates. These homologs have been shown to have lower K_Ms, which is sometimes thought of as having improved substrate binding (Figure 3A).[26] We identified four residues within the active site entry gate of these homologous ADA2s that were more hydrophobic than the *Homo sapiens* ADA2: E182, R222, S265, H267, which may be responsible for the difference in their respective K_Ms (Figure 3B and C).[26] AlphaFold-predicted structural

Table 1. SignalP and DeepLoc predictions of SSPs' performance with ADA1

SSP	SignalP	DeepLoc
PROS	96%	80%
RNAS4	84%	90%
CLM9	73%	95%
CCL22	84%	82%
GRAB	98%	67%
IgKCm	90%	75%
HSA	81%	78%
CATE	60%	97%
IL19	46%	85%
CD177	98%	4%
ADA2	59%	2%
IL2	53%	0%
CYXL	26%	0%
None	0	0

The middle column shows predicted SignalP cleavage efficiency and the right column shows the predicted DeepLoc extracellular probability.
ADA1, adenosine deaminase 1; SSP, secretory signal peptides.

comparisons of *H. sapiens* ADA2 and the lowest K_M and most hydrophobic homolog, *Sarcophaga peregrina,* also show the active site to be considerably more accessible with a larger entry gate (Figure 3B and Supplementary Figure S5, available at https://doi.org/10.1016/j.iotech.2023.100394).[42] In addition, prior work has demonstrated that a ADA2 variant with R222Q and S265N mutations exhibited a superior K_M (∼1 mM) and k_{cat} (169 s^{-1}) and could slow tumor growth in mice.[33]

Guided by our phylogenetic comparison, we constructed a degenerate library of ADA2 variants that would allow for introduction of more hydrophobic residues. Using overlap extension PCR and primer-mediated introduction of nucleotide diversity at positions E182 (E, G, M, V), R222 (R, S, T, Q), S265 (S, A, T, N), and H267 (H, I, V, D), we constructed a library of up to 256 ADA2 variants that we ligated into a pcDNA3 backbone flanked by T2A-GLuc via Golden Gate assembly (Figure 3D).

To screen our library at high throughput, we developed a reverse transfection screening technique for HEK293T cells in 96-well plates (Supplementary Figure S6, available at https://doi.org/10.1016/j.iotech.2023.100394). Forty-eight hours after transfection, we tested cell culture supernatant for ADA activity and GLuc luminescence. We tested ∼300 ADA2 variants, and promisingly, 24% had improved extracellular ADA activity than wild-type ADA2 (Figure 4A). To account for potential variability during our screen, we selected the top 20 variants by ADA activity, rescreened them in sextuplet, and sequenced them to determine their mutational profile (Figure 4B, Supplementary Table S2, available at https://doi.org/10.1016/j.iotech.2023.100394). As expected, all 20 variants had at least one mutation, and the top performing ADA2v20 variant (ADA2-R222T/S265A) exhibited an approximate 30-fold increase in ADA activity compared to the wild-type enzyme (Figure 4B). We isolated this variant twice, as variant 18 also contained the same sequence and a similar fold change adenosine degradation rate (∼20×). Interestingly, this variant also had the same residues at positions 222 and 265 as two homologs from *Lutzomyia longipalpis and S. peregrina* (Figure 3A). We also recovered the previously described ADA2-R222Q/S265N variant from our library, but found that it exhibited only an ∼9× increase in adenosine degradation activity at our tested conditions (adding 250 μM adenosine to cell culture supernatant). In summary, we successfully engineered the ADA2 binding pocket to be more hydrophobic and accessible (Supplementary Figure S7, available at https://doi.org/10.1016/j.iotech.2023.100394), and our highest activity variant exhibited a 20- to 30-fold increase in adenosine degradation rate compared to wild-type enzyme and an ∼4-fold increase in extracellular degradation compared to ADA1.[43] In addition, the ADA2v20 variant retained its native secretion capacity, as confirmed via western blot (Supplementary Figure S2, available at https://doi.org/10.1016/j.iotech.2023.100394). ADA2v20 also showed greatly enhanced extracellular activity compared to ADA2wt and ADA1 across a broader range of substrate concentrations (62.5 μM, 125 μM, and 250 μM adenosine) (Figure 4C). At 62.5 μM, ADA2v20 outperformed ADA2wt by ∼35-fold and at 125 μM ADA2v20 outperformed it by ∼50-fold. Notably, ADA2v20 also outperforms the previously reported ADA2-R222Q/S265N variant across this same adenosine concentration range (Supplementary Figure S8, available at https://doi.org/10.1016/j.iotech.2023.100394).[33]

Purification and kinetic characterization of the engineered ADA2v20 enzyme

To precisely ascertain the kinetic parameters of ADA2v20, we expressed the variant in HEK293T cells through transient transfection, media were changed after 24 h to serum-free media to reduce protein impurities in the supernatant (namely bovine serum albumin), and then purified the ADA2v20 from supernatant using fast pressure liquid chromatography. We expressed and purified the ADA2wt protein for comparison. Both enzymes were >95% pure and exhibited glycosylation heterogeneity, as determined by SDS-PAGE (Supplementary Figure S9, available at https://doi.org/10.1016/j.iotech.2023.100394). Using a time-coursed kinetic assay, we determined the Michaelis–Menten kinetic parameters of ADA2wt (k_{cat} = 30 s^{-1}, K_M = 2.2 mM), which is consistent with previously reported kinetic parameters of ADA2wt (k_{cat} = 45-88 s^{-1} K_M = 2.25-4.4 mM), and ADA2v20 (k_{cat} = 30 s^{-1}, K_M = 0.326 mM) (Figure 4D).[26,33] Thus, we improved the K_M of ADA2wt approximately sevenfold, while preserving its high k_{cat}.

ADA2 variant 20 is readily secreted by HEK293T, Jurkat, and CAR T cells

In HEK293T cells, ADA2v20 exhibited a 3.75-fold increase in extracellular adenosine degradation rate compared to ADA1, and a >30× increase in ADA activity compared to ADA2wt (Figure 5A). To ascertain expression levels in an engineered T cell, we first engineered Jurkat T cells with a control tagBFP vector or ADA2v20 to compare their adenosine degradation rates. Forty-eight hours post-transduction, we sorted

A

Species	K_M (μM)	Residue 182	Residue 222	Residue 265	Residue 267
H. sapiens	2228	E	R	S	H
G. gallus	150	E	I	A	H
X. laevis	150	E	M	T	H
P. falciparum	88	V	S	T	D
L. longipalpis	50	G	T	A	V
S. peregrina	15	G	T	A	I

B

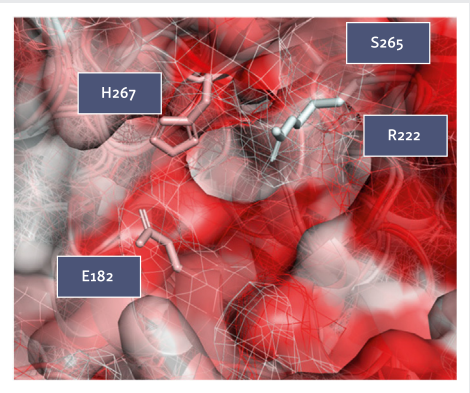

C

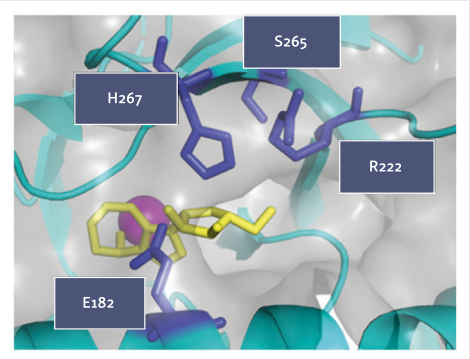

D

Residue 182	Residue 222	Residue 265	Residue 267
E	R	S	H
G	T	A	I
M	S	T	V
V	Q	N	D

Figure 3. Hydrophilic adenosine deaminase 2 (ADA2) residues selected for mutagenesis to improve activity. (A) ADA2 entry gate residue comparison between *Homo sapiens* and phylogenetic homologs. (B) AlphaFold structural prediction of ADA2wt (mesh) and *Sarcophaga peregrina* ADA2 (surface) without docked ligand colored for hydrophobicity using PyMOL color h function. Deeper red indicates more hydrophobic residues and the sticks correspond to ADA2wt residues. (C) PDB 3lgg ribbon depiction of the ADA2 hydrophilic residues selected for mutagenesis at the entry gate of the active site. Purple sticks represent the amino acids selected for mutagenesis, the yellow molecule is an adenosine analog (coformycin), and the pink circle is the coordinating zinc ion. (D) Positional possibilities for ADA2 within the library. Bold letters represent the wild-type residues.

tagBFP+ cells by fluorescence-activated cell sorting. We then seeded 10^6 cells/ml and sampled their culture supernatant for ADA activity assays. Though Jurkat background is higher due to considerable ADA1 expression, ADA2v20-expressing Jurkat cells still exhibited a 27-μM/h relative increase in adenosine degradation rate (Figure 5B).[44]

Next, we tested if ADA2v20-engineered CAR T cells could degrade a clinically relevant amount of adenosine *in vitro*. To evaluate the performance of ADA2v20-engineered CAR T cells, we transduced primary murine T cells with either just an aMUC16^{ecto} CAR or with one of three ADA enzymes, ADA1, ADA2wt, or ADA2v20. We achieved sufficient transduction efficiencies (Figure 5C).[4] CAR T cells engineered to secrete ADA2v20 were able to degrade an additional 30 μM/h of adenosine *in vitro,* while adenosine degradation of CAR only-, ADA1-, and ADA2wt-engineered CAR T cells was undetectable (Figure 5D).

DISCUSSION

Enzyme-mediated depletion of tumor accumulated immunosuppressive metabolites can stimulate antitumor immune responses or even augment established checkpoint inhibitors (e.g. PD-1 and CTLA-4).[33,45,46] Here, we present an approach for immunosuppressive metabolite (adenosine) depletion mediated by CAR T-cell therapies. We evolved a novel ADA2 enzyme variant for this application that is more considerably more active at tumoral adenosine concentrations than the wild-type enzyme, and we demonstrated that CAR T cells secreting this engineered ADA2 variant can degrade relevant amounts of adenosine.

This treatment modality may provide a path forward to improve the efficacy of CAR T-cell therapies, specifically by resisting adenosine-mediated immune suppression. In two separate recent studies, CRISPR-Cas9-mediated $A_{2A}R$ knockout and genetic ADA1 overexpression were shown to improve the function of CAR T-cell therapies by mitigating T-cell susceptibility to adenosine suppression.[18,47] These attempts may have been limited in their impact because adenosine could still signal through the $A_{2B}R$ on $A_{2A}R-/-$ T cells and the extent to which ADA1-overexpressing T cells secreted ADA1 and degraded extracellular adenosine (to prevent its interaction with adenosine receptors (ARs)) was unclear. Notably, the IL-2 SSP that was fused to ADA1 in this study decreased ADA1 secretion by ~75% in our hands (Figure 2D). Indeed, it is possible that the internal metabolic consumption of adenosine by ADA1 could rescue CAR T-cell function *in vivo*.[47] Our demonstrated approach to secrete ADA2 from engineered cells to degrade extracellular adenosine may be more promising than these prior attempts as ADA2 can thus prevent adenosine from binding to any adenosine receptor through its conversion into inosine, while not potentially altering intracellular CAR T-cell nucleoside metabolism. Our approach could theoretically invigorate bystander immune cells as well. So-called 'armored' CAR T-cell therapies that prevent immune suppression in an autocrine and paracrine manner were recently shown for PD-1-blocking scFv secretion.[4] Both Jurkat and primary T cells

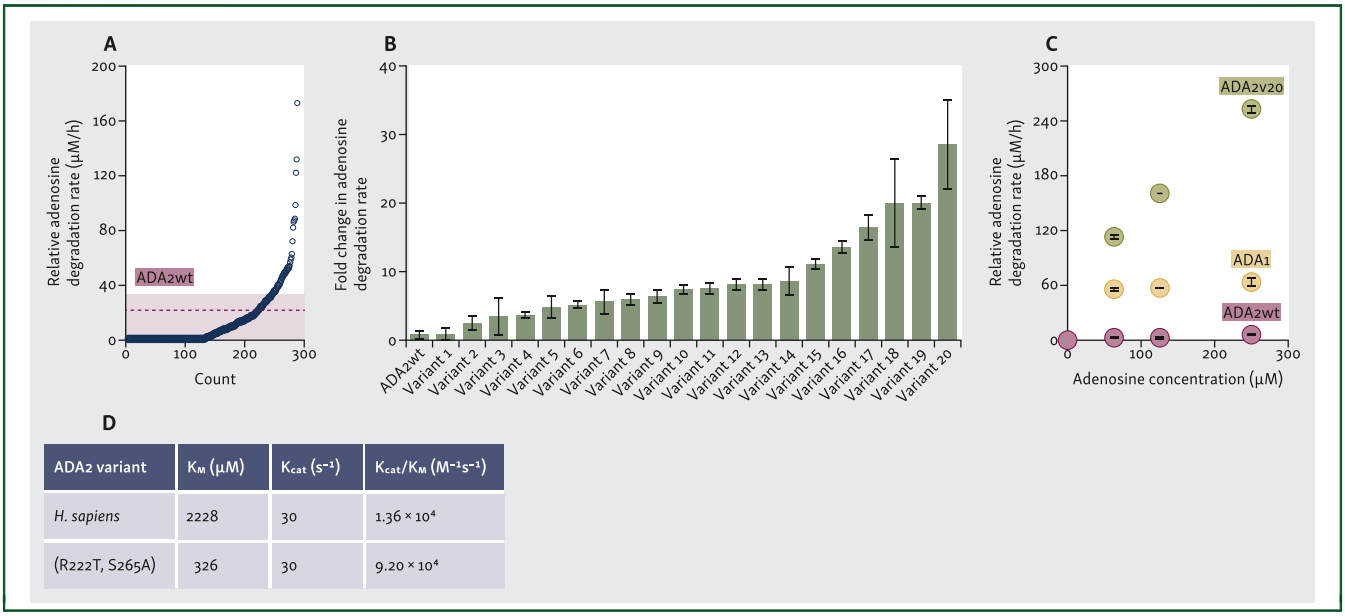

Figure 4. High-throughput screening of adenosine deaminase 2 (ADA2) library. (A) Library performance by relative adenosine degradation rate (subtracting the background adenosine degradation of non-transfected 293T control). Each point represents an ADA2 variant within the library. The thick red dashed line represents the mean ADA2wt transfection performance. The red dotted line and shading represent standard error of the mean (SEM) of ADA2wt ($n = 12$). (B) The top 20 candidates from (A), as adenosine degradation rate normalized by Gaussia luciferase (GLuc), were rescreened in replicate, $n = 6$. Bars represent the mean fold change in adenosine degradation rate compared to wild-type ADA2 and error bars represent SEM. (C) ADA2v20 outperforms ADA1 and ADA2wt over a range of adenosine concentrations. Green points represent ADA2v20, orange points represent ADA1, and red points represent ADA2wt. Each point represents the mean relative adenosine degradation, $n = 3$, errors bars = SEM. (D) Table depicting the kinetic parameters of purified ADA2wt and ADA2v20 (i.e. R222T, S265A).

engineered to express our evolved ADA2v20 could degrade significant amounts of adenosine *in vitro* extracellularly. In the future, head-to-head comparisons of ADA2-secreting versus ADA1-overexpressing CAR T cells can glean insights into the optimal route of enzymatic adenosine degradation to enhance antitumor immunity.

A question remains whether cellular secretion of ADA1 is possible, but perhaps future approaches could exploit unconventional (i.e. signal peptide independent) mechanisms of secretion.[48] Our results show that researchers should exercise caution when relying on *in silico* algorithms like DeepLoc and SignalP to predict protein secretion, whose fidelity may not be reliable for transgenic or 'engineered' constructs. There also may be other avenues to enable secretion of ADA1. The fusion of other molecular chaperones (e.g. apart from those tested here) could facilitate cellular secretion, for instance, the fusion of ADA1 with ADA2v20/ADA2wt or other serum-resident proteins. Future

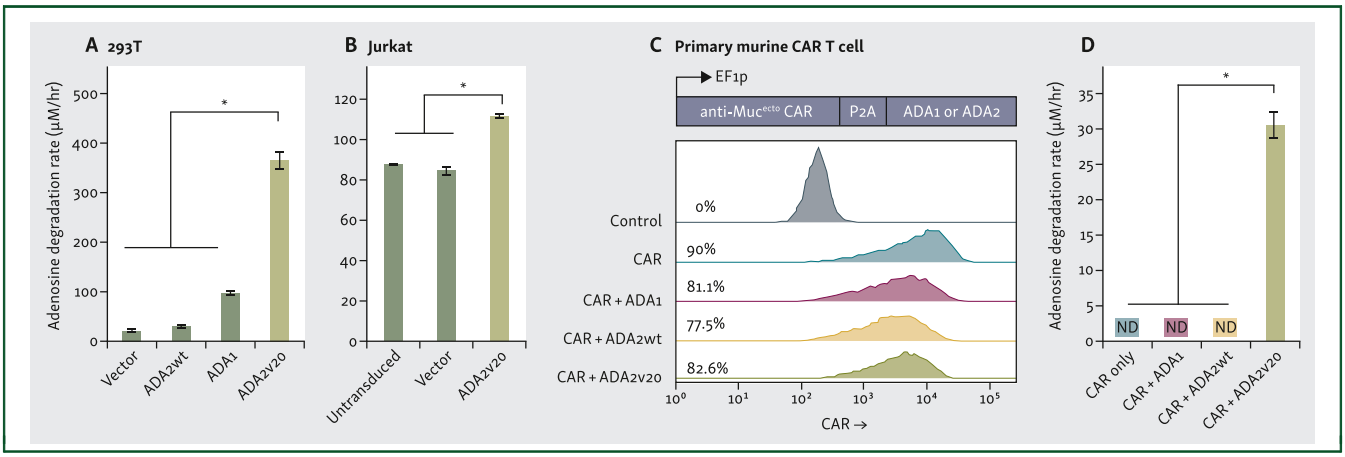

Figure 5. ADA2v20 performance in engineered cell lines. (A) Adenosine degradation rate by ADA2wt, ADA1, and ADA2v20 in HEK293T cells 48 h post-transfection. Bars represent means of $n = 3$ experimental replicates, error bars are standard error of the mean (SEM). (B) Adenosine degradation rate mediated by the secreted ADA2v20 in stably transduced Jurkat T cells subtracted from media background. Bars represent mean of $n = 3$ replicates and error bars are SEM. (C) Construct depiction that shows how the EF1α promoter drives expression of the αMUC16^{ecto} chimeric antigen receptor (CAR), as well as a P2A allowing for co-expression of ADA1, ADA2wt, or ADA2v20. Below the construct depiction are the transduced CAR T cells stained to evaluate the transduction efficiencies. The data were analyzed in Flowjo. (D) Adenosine degradation rates mediated by the murine T cells expressing CAR only, CAR + ADA1, CAR + ADA2wt, or CAR + ADA2v20. Primary CAR T cells were seeded at constant cellular density and sampled 48 h later for supernatant adenosine degradation rate, while subtracting background media activity. ND, not detected. Bars represent mean of $n = 3$ experimental replicates and error bars represent SEM. *$P < 0.01$ by Tukey's honestly significant difference (HSD) test.

protein engineering efforts could also shuffle key catalytic domains of ADA1 into ADA2 to impart the desirable activity of ADA1 with secretion capabilities.[49]

The primary issue limiting the utility of ADA2 for systemic adenosine depletion in tumors (mediated by T cells) was its poor activity at lower concentrations, a property that we showed could be improved by lowering its K_M through targeted mutagenesis. ADA1 activity is still superior to ADA2v20, though the variant that we have engineered here is secreted more efficiently and thus considerably more effective at degrading extracellular adenosine in engineered cells than ADA1 and ADA2wt at micromolar (tumoral) concentrations.

In summary, we have engineered an improved ADA2 variant for adenosine depletion in the solid tumor microenvironment and showed that it is secreted by mammalian cells and significantly more active than the wild-type enzyme at tumoral adenosine concentrations. Finally, we carried out *in vitro* studies to demonstrate the feasibility for CAR T cells to secrete this enzyme, setting the stage to be incorporated into a suitable CAR T-cell therapy model for preclinical study. In the future, we aim to demonstrate the capability of our engineered T cells to resist adenosine-mediated immune suppression both *in vitro* and *in vivo*.

ACKNOWLEDGEMENTS

The authors acknowledge Dr Susan Thomas (BMED, Georgia Tech) for graciously providing Jurkat cells and Dr Gabe Kwong (BMED, Georgia Tech) for providing HEK293T cells and assistance in primary T-cell isolation and culture. The authors also thank Dr Andrés García (ME, Georgia Tech) for assistance with western blot protocols.

FUNDING

This work was supported by the National Institutes of Health [grant number 1DP2CA280622-01 to JB].

DISCLOSURE

JB and JRC have filed patent applications related to this work. All other authors have declared no conflicts of interest.

REFERENCES

1. D'Aloia MM, Zizzari IG, Sacchetti B, Pierelli L, Alimandi M. CAR-T cells: the long and winding road to solid tumors. *Cell Death Dis*. 2018;9(3):282.
2. Rafiq S, Hackett CS, Brentjens RJ. Engineering strategies to overcome the current roadblocks in CAR T cell therapy. *Nat Rev Clin Oncol*. 2020;17(3):147-167.
3. Cox JR, Blazeck J. Protein engineering: a driving force toward synthetic immunology. *Trends Biotechnol*. 2022;40(4):509-521.
4. Rafiq S, Yeku OO, Jackson HJ, et al. Targeted delivery of a PD-1-blocking ScFv by CAR-T cells enhances anti-tumor efficacy in vivo. *Nat Biotechnol*. 2018;36(9):847-856.
5. Yeku OO, Purdon TJ, Koneru M, Spriggs D, Brentjens RJ. Armored CAR T cells enhance antitumor efficacy and overcome the tumor microenvironment. *Sci Rep*. 2017;7(1):10541.
6. Avanzi MP, Yeku O, Li X, et al. Engineered tumor-targeted T cells mediate enhanced anti-tumor efficacy both directly and through activation of the endogenous immune system. *Cell Rep*. 2018;23(7):2130-2141.
7. Li X, Daniyan AF, Lopez AV, Purdon TJ, Brentjens RJ. Cytokine IL-36γ improves CAR T-cell functionality and induces endogenous antitumor response. *Leukemia*. 2021;35(2):506-521.
8. Sitkovsky MV, Hatfield S, Abbott R, Belikoff B, Lukashev D, Ohta A. Hostile, hypoxia—A2-adenosinergic tumor biology as the next barrier to overcome for tumor immunologists. *Cancer Immunol Res*. 2014;2(7):598-605.
9. Ohta A, Sitkovsky M. Role of G-protein-coupled adenosine receptors in downregulation of inflammation and protection from tissue damage. *Nature*. 2001;414(6866):916-920.
10. Ohta A, Gorelik E, Prasad SJ, et al. A2A adenosine receptor protects tumors from antitumor T cells. *Proc Natl Acad Sci U S A*. 2006;103(35):13132-13137.
11. Fong L, Hotson A, Powderly JD, et al. Adenosine 2A receptor blockade as an immunotherapy for treatment-refractory renal cell cancer. *Cancer Discov*. 2020;10(1):40-53.
12. Jennings MR, Munn D, Blazeck J. Immunosuppressive metabolites in tumoral immune evasion: redundancies, clinical efforts, and pathways forward. *J Immunother Cancer*. 2021;9(10):e003013.
13. Deaglio S, Dwyer KM, Gao W, et al. Adenosine generation catalyzed by CD39 and CD73 expressed on regulatory T cells mediates immune suppression. *J Exp Med*. 2007;204(6):1257-1265.
14. Stagg J, Divisekera U, McLaughlin N, et al. Anti-CD73 antibody therapy inhibits breast tumor growth and metastasis. *Proc Natl Acad Sci U S A*. 2010;107(4):1547-1552.
15. Allard B, Pommey S, Smyth MJ, Stagg J. Targeting CD73 enhances the antitumor activity of anti-PD-1 and anti-CTLA-4 MAbs. *Clin Cancer Res*. 2013;19(20):5626-5635.
16. Young A, Ngiow SF, Barkauskas DS, et al. Co-inhibition of CD73 and A2AR adenosine signaling improves anti-tumor immune responses. *Cancer Cell*. 2016;30(3):391-403.
17. Sitkovsky MV. Lessons from the A2A adenosine receptor antagonist-enabled tumor regression and survival in patients with treatment-refractory renal cell cancer. *Cancer Discov*. 2020;10(1):16-19.
18. Giuffrida L, Sek K, Henderson MA, et al. CRISPR/Cas9 mediated deletion of the adenosine A2A receptor enhances CAR T cell efficacy. *Nat Commun*. 2021;12(1):3236.
19. Welihinda AA, Kaur M, Greene K, Zhai Y, Amento EP. The adenosine metabolite inosine is a functional agonist of the adenosine A2A receptor with a unique signaling bias. *Cell Signal*. 2016;28(6):552-560.
20. Chen J, Chaurio RA, Maueröder C, et al. Inosine released from dying or dead cells stimulates cell proliferation via adenosine receptors. *Front Immunol*. 2017;8:504.
21. Mabley JG, Rabinovitch A, Suarez-Pinzon W, et al. Inosine protects against the development of diabetes in multiple-low-dose streptozotocin and nonobese diabetic mouse models of type 1 diabetes. *Mol Med*. 2003;9(3):96-104.
22. Haskó G, Kuhel DG, Németh ZH, et al. Inosine inhibits inflammatory cytokine production by a posttranscriptional mechanism and protects against endotoxin-induced shock. *J Immunol*. 2000;164(2):1013-1019.
23. Mager LF, Burkhard R, Pett N, et al. Microbiome-derived inosine modulates response to checkpoint inhibitor immunotherapy. *Science*. 2020;369(6510):1481-1489.
24. Wang T, Gnanaprakasam JNR, Chen X, et al. Inosine is an alternative carbon source for $CD8^+$-T-cell function under glucose restriction. *Nat Metab*. 2020;2(7):635-647.
25. Ma MT, Jennings MR, Blazeck J, Lieberman RL. Catalytically active holo Homo sapiens adenosine deaminase I adopts a closed conformation. *Acta Crystallogr D Struct Biol*. 2022;78(1):91-103.
26. Zavialov AV, Yu X, Spillmann D, Lauvau G, Zavialov AV. Structural basis for the growth factor activity of human adenosine deaminase ADA2. *J Biol Chem*. 2010;285(16):12367-12377.
27. Cortés A, Gracia E, Moreno E, et al. Moonlighting adenosine deaminase: a target protein for drug development. *Med Res Rev*. 2015;35(1):85-125.
28. Martinez-Navio JM, Casanova V, Pacheco R, et al. Adenosine deaminase potentiates the generation of effector, memory, and regulatory CD4+ T cells. *J Leukoc Biol*. 2011;89(1):127-136.

29. Ginés S, Mariño M, Mallol J, et al. Regulation of epithelial and lymphocyte cell adhesion by adenosine deaminase-CD26 interaction. *Biochem J*. 2002;361(Pt 2):203-209.
30. Zavialov AV, Gracia E, Glaichenhaus N, Franco R, Zavialov AV, Lauvau G. Human adenosine deaminase 2 induces differentiation of monocytes into macrophages and stimulates proliferation of T helper cells and macrophages. *J Leukoc Biol*. 2010;88(2):279-290.
31. Tiwari-Heckler S, Yee EU, Yalcin Y, et al. Adenosine deaminase 2 produced by infiltrative monocytes promotes liver fibrosis in nonalcoholic fatty liver disease. *Cell Rep*. 2021;37(4):109897.
32. Sitkovsky MV, Ohta A. Methods for using extracellular adenosine inhibitors and adenosine receptor inhibitors to enhance immune response and inflammation. US8716301B2; May 6, 2014. Available at https://patents.google.com/patent/US8716301B2/en. Accessed March 28, 2023.
33. Wang L, Londono LM, Cowell J, et al. Targeting adenosine with adenosine deaminase 2 to inhibit growth of solid tumors. *Cancer Res*. 2021;81(12):3319-3332.
34. Sarkar OS, Donninger H, Rayyan NA, et al. Monocytic MDSCs exhibit superior immune suppression via adenosine and depletion of adenosine improves efficacy of immunotherapy. *Sci Adv*. 2023;9(26):eadg3736.
35. Dunwiddie TV, Masino SA. The role and regulation of adenosine in the central nervous system. *Annu Rev Neurosci*. 2001;24:31-55.
36. Green MR, Sambrook J, Sambrook J. *Molecular Cloning: A Laboratory Manual*. 4th ed. Cold Spring Harbor, NY: Cold Spring Harbor Laboratory Press; 2012.
37. Owji H, Nezafat N, Negahdaripour M, Hajiebrahimi A, Ghasemi YA. Comprehensive review of signal peptides: structure, roles, and applications. *Eur J Cell Biol*. 2018;97(6):422-441.
38. Güler-Gane G, Kidd S, Sridharan S, Vaughan TJ, Wilkinson TCI, Tigue NJ. Overcoming the refractory expression of secreted recombinant proteins in mammalian cells through modification of the signal peptide and adjacent amino acids. *PLoS One*. 2016;11(5):e0155340.
39. Almagro Armenteros JJ, Sønderby CK, Sønderby SK, Nielsen H, Winther O. DeepLoc: prediction of protein subcellular localization using deep learning. *Bioinformatics*. 2017;33(21):3387-3395.
40. Almagro Armenteros JJ, Tsirigos KD, Sønderby CK, et al. SignalP 5.0 improves signal peptide predictions using deep neural networks. *Nat Biotechnol*. 2019;37(4):420-423.
41. Jefferis R. Glycosylation as a strategy to improve antibody-based therapeutics. *Nat Rev Drug Discov*. 2009;8(3):226-234.
42. Jumper J, Evans R, Pritzel A, et al. Highly accurate protein structure prediction with AlphaFold. *Nature*. 2021;596:583-589.
43. Zhu C, Gao Y, Li H, et al. Characterizing hydrophobicity of amino acid side chains in a protein environment via measuring contact angle of a water nanodroplet on planar peptide network. *Proc Natl Acad Sci U S A*. 2016;113(46):12946-12951.
44. Kainthla RP, Kashyap RS, Prasad S, Purohit HJ, Taori GM, Daginawala HF. Evaluation of adenosine deaminase assay for analyzing t-lymphocyte density in vitro. *In Vitro Cell Dev Biol Anim*. 2006;42(10):287-289.
45. Triplett TA, Garrison KC, Marshall N, et al. Reversal of indoleamine 2,3-dioxygenase-mediated cancer immune suppression by systemic kynurenine depletion with a therapeutic enzyme. *Nat Biotechnol*. 2018;36(8):758-764.
46. Blazeck J, Karamitros CS, Ford K, et al. Bypassing evolutionary dead ends and switching the rate-limiting step of a human immunotherapeutic enzyme. *Nat Catal*. 2022;5(10):952-967.
47. Qu Y, Dunn ZS, Chen X, et al. Adenosine deaminase 1 overexpression enhances the antitumor efficacy of chimeric antigen receptor-engineered T cells. *Hum Gene Ther*. 2022;33(5-6):223-236.
48. Rabouille C. Pathways of unconventional protein secretion. *Trends Cell Biol*. 2017;27(3):230-240.
49. Meyer MM, Silberg JJ, Voigt CA, et al. Library analysis of SCHEMA-guided protein recombination. *Protein Sci*. 2003;12(8):1686-1693.